Calibration and Test Bed Simulation of a 40cm^2 CPTU Cone

Erick Baziw

Baziw Consulting Engineers Ltd., Vancouver B.C., Canada
ebaziw@bcengineers.com

ABSTRACT

In cone penetration testing (CPT) an electronic penetrometer is pushed at a constant rate into penetrable soils and cone bearing (q_c), sleeve friction (f_c) and dynamic pore pressure (u) are recorded with depth. The measured q_c, f_s and u values are utilized to estimate soil type and associated properties. Cone tips have areas which vary from 5cm^2 to 40 cm^2. The larger tips allow for the penetration of gravely soils while small cone tips are utilized for shallow soil investigations. The measured cone bearing and sleeve friction values are blurred or averaged. The measurements are also susceptible to anomalous peaks and troughs due to the relatively small diameter cone tip penetrating sandy, silty and gravelly soils. The cones with relatively smaller cone tips are significantly more susceptible to the anomalous peaks and troughs while the cones with larger cone tips are more susceptible to the smoothing of the cone tip and sleeve friction measurements. Baziw Consulting Engineers (BCE) has invested considerable resources in addressing the q_c and f_s measurements distortions. This paper outlines the techniques developed by BCE and integrates them so that optimal soil properties can be obtained from CPT data sets. Particular focus is put on relatively larger cone tips because they can penetrate soils with high resistance and are less susceptible to the additive measurement noise of anomalous peaks and troughs. The anomalous peaks and troughs are more challenging to remove or minimize than the q_c and f_s blurring effects. It is of paramount importance to first implement newly developed signal processing and optimal estimation algorithms on extensive test bed simulations prior to processing real data sets. This paper also outlines the results from processing a challenging test bed simulation of a 40 cm^2 cone tip data set with BCE's newly developed algorithms.

Keywords: cone penetration testing (CPT); optimal estimation; test bed simulation; Monte Carlo techniques.

1. Introduction

The Cone Penetration Test (CPT) is an extensively utilized geotechnical in-situ tool which allows for the identification and characterization of sub-surface soils (Lunne et al., 1997; Robertson, 1990; ASTM D6067, 2017). In CPT a steel cone with electronic sensors is pushed vertically into the ground at a typical standard rate of 2 cm per second. The cone penetrometer has electronic sensors to measure penetration resistance at the tip (q_c) and friction in the shaft (f_s) during penetration. A CPT probe equipped with a pore-water pressure sensor is called a piezo-cone (CPTU cones). For piezo-cones with the filter element right behind the cone tip (the so-called u_2 position) it is standard practice to correct the recorded tip resistance and sleeve friction for the measured pore pressure. This corrected cone tip resistance is normally referred to as q_t.

The two most commonly utilized penetrometers have cone tips with associated areas of 10 cm^2 and 15 cm^2. Larger cone tip penetrometers (33 cm^2 and 40 cm^2) are utilize to penetrate gravely soils. Small cone tips (2 cm^2 and 5 cm^2) are utilized for shallow soil investigations. Figure 2 illustrates the comparable size of cone tips with areas of 5 cm^2, 10 cm^2, 15 cm^2 and 40 cm^2.

CPT soil classification entails grouping soils according to their engineering behavior (i.e., Soil Behavior Type (SBT)). This is accomplished by empirically relating measured cone sensor data to type of

Figure 1. 5 cm^2, 10 cm^2, 15 cm^2 and 40 cm^2 penetrometers (Robertson and Cabal, 2012).

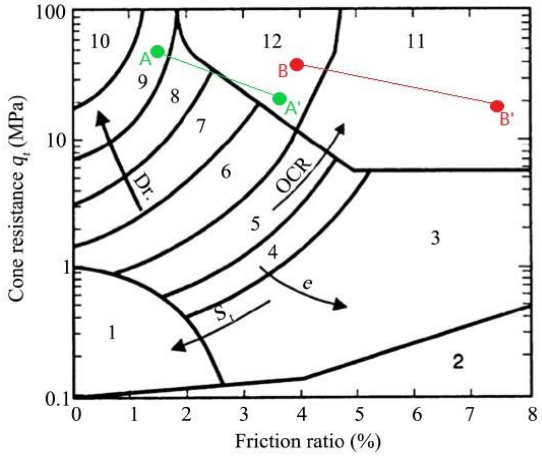

Zone	Soil Behavior Type
1	*Sensitive fine grained*
2	*Organic material*
3	*Clay*
4	*Silty Clay to clay*
5	*Calyey silt to silty clay*
6	*Sandy silt to clayey silt*
7	*Silty sand to sandy silt*
8	*Sand to silty sand*
9	*Sand*
10	*Gravelly sand to sand*
11	*Very stiff fine grained*
12	*Sand to clayey sand*

**Overconsolidated or cemented*

Figure 2. SBT chart based on CPTU cone resistance, q_t, and friction ratio, R_f (where $R_f = (f_s/q_c)100\%$) (Robertson et al., 1986).

soil in SBT charts. A commonly utilized CPT/CPTU SBT chart is based on q_t and friction ratio, R_f [where: $R_f = (f_s/q_c)100\%$] (Robertson et al., 1986) measurements. Figure 2 illustrates a SBT chart where 12 soil types are identified. For accurate CPT/CPTU soil classifications it is of paramount importance that cone bearing measurements of q_c and f_s with minimal distortions and added measurement errors are obtained.

Both cone bearing and sleeve friction measurements obtain smoothed/averaged estimates of the true values; Furthermore, the measurements are susceptible to anomalous peaks and troughs due to the relatively small diameter cone tip penetrating sandy, silty and gravelly soils (Lunne et. al, 1997; Baziw, E. and Verbeek, 2021a). The „high" peaks result from the penetration of interbedded gravels and stones and the "low" troughs results from the penetration of softer materials or local pore pressure build-up. It has been found that the anomalous peaks and troughs can be comparatively more challenging to remove or minimize than the smoothing effects.

Cones with relatively smaller cone tips are significantly more susceptible to the anomalous peaks and troughs while cones with relatively larger tips are more susceptible to the smoothing effect. BCE has invested considerable resources in designing optimal estimation algorithms for minimizing the effects of cone tip blurring (*qcHMM* and *CPSPE* algorithms), cone sleeve blurring (*OSFE_IFM* algorithm), and anomalous peak and troughs (*qcKF* algorithm). This paper briefly outlines the *qcHMM*, *CPSPE* and *CPSPE* algorithms and incorporates them in a very challenging test bed simulation for a 40 cm^2 cone. The 40 cm^2 cone was selected because it is relatively less susceptible to anomalous peak and troughs and it can be utilized to penetrate very stiff soils.

The design and implementation of sophisticated optimal estimation algorithms (OEAs) for analyzing geotechnical in-situ data has gain significantly popularity in recent years. Unfortunately, many of the newly developed algorithms do not carry out sufficient challenging test bed simulations for algorithm verification. Thorough test bed simulation and analysis is required prior to implementation of OEAs on real data sets. This is the motivation to firstly demonstarte the efficacy of the *qcHMM*, *CPSPE*, and *OSFE-IFM* algorithms with challenging test bed simulations.

2. CPT measurement models and optimal estimation algorithms

The CPT cone bearing and sleeve friction measurements provide blurred\averaged estimates of the true values. This section describes the blurring mathematical details and the associated OEAs.

2.1. Cone bearing measurements

2.1.1. Cone bearing governing equations

The cone tip resistance measured at a particular depth is affected by the values above and below the depth of interest which results in an averaging or blurring of the true values (q_v) values (Boulanger and DeJong, 2018; Baziw and Verbeek, 2021b, 2022a, 2022b). The blurring of cone bearing measurements is especially of concern when mapping thin soil layers (e.g., liquefaction assessment). Mathematically the measured cone tip resistance q_c is described as

$$q_c(d) = \sum_{j=1}^{N\times\left(\frac{d_c}{\Delta}\right)} w_c(j) \times q_v(\Delta_{qc} + j) + v(d) \quad (1)$$
$$\Delta_{qc} = (d - \Delta_{wc}),\ \ \Delta_{wc} = N \times \left(\frac{d_c}{2\Delta}\right)$$

where

- d the cone depth
- dc the cone tip diameter
- Δ_{qc} the q_c sampling rate
- $q_c(d)$ the measured cone penetration tip resistance
- $q_v(d)$ the true cone penetration tip resistance
- $w_c(d)$ the $q_v(d)$ blurring function
- $v(d)$ additive noise (anomalous "peak" and "troughs"

The governing equations for w_c are outlined below:

$$w_c = \frac{w_1 w_2}{\sum w_1 w_2} \quad (2a)$$

$$w_1 = \frac{C_1}{1 + \left|\left(\frac{z'}{z'_{50}}\right)^{m_z}\right|} \quad (2b)$$

$$z' = \frac{z - z_{tip}}{d_c} \quad (2c)$$

$$C_1 = 1\ for\ z' \geq 0$$
$$= 1 + \frac{z'}{8}\ for\ -4 \leq z' < 0 \quad (2d)$$
$$= 0.5\ for\ z' < -4$$

$$z'_{50} = 1 + 2\left(C_2 z'_{50,ref} - 1\right) \times \left[1 - \frac{1}{1+\left(\frac{q_{v,z'=0}}{q_{v,z'}}\right)^{m_{50}}}\right] \quad (2e)$$

$$C_2 = 1\ for\ z' > 0$$
$$= 0.8\ for\ z' \leq 0 \quad (2f)$$

$$w_2 = \sqrt{\frac{2}{1 + \left(\frac{q_{v,z'}}{q_{v,z'=0}}\right)^{m_q}}} \quad (2g)$$

where

- w_1 accounts for the relative influence of any soil decreasing with increasing distance from the cone tip.
- w_2 adjusts the relative influence that soils away from the cone tip will have on the penetration resistance based on whether those soils are stronger or weaker.
- z' the depth relative to the cone tip normalized by the cone diameter.

In general terms, soils in front of the cone tip have a greater influence on penetration resistance than the soils behind the cone tip. The four main parameters which influence w_c are $z'_{50,ref}$, m_z, m_{50}, and m_q. Boulanger and DeJong (Boulanger and DeJong, 2018) outline the baseline values for these parameters as $z'_{50,ref} = 4.0$, $m_z = 3.0$, $m_{50} = 0.5$, and $m_q = 2$. Boulanger and DeJong also set $N = 60$ in eq. (1) (i.e., $-30 \leq z' \leq 30$). The value of N = 60 cone diameters was implemented due to w_c being close to zero for distance exceeding 30 cone diameters from the cone tip based upon the previously specified baseline cone smoothing parameters.

2.1.2. *q_cHMM* algorithm

The *q_cHMM* algorithm (Baziw and Verbeek, 2021b, 2022a, and 2022b) was developed to address the smoothing/averaging of cone bearing measurements. This algortim utilizes the Bayesian recursive estimation (BRE) (Arulampalam et. al, 2002) Hidden Markov Model (HMM) filter. The HMM filter (also termed a grid-based filter) has a discrete state-space representation and has a finite number of states. In the HMM filter the posterior PDF is represented by the delta function approximation as follows:

$$p(x_{k-1}|z_{1:k-1}) = \sum_{i=1}^{N_s} w^i_{k-1\backslash k-1}\delta\left(x_{k-1} - x^i_{k-1}\right) \quad (3)$$

where x^i_{k-1} and $w^i_{k-1|k-1}$, $i = 1,\ldots,N_s$, represent the fixed discrete states and associated conditional probabilities, respectively, at time index *k-1*, and N_s the number of particles utilized. In the case of the *q_cHMM* algorithm the HMM discrete states represent possible q_v values where maximum, minimum and resolution values are specified. The HMM governing equations are outlined in Table 1.

Table 1. HMM Filtering Algorithm

Step	Description	Mathematical Representation
1	Initialization (k=0) – initialize particle weights.	e.g., $w^i_k \sim 1/N_s$, $i = 1,\ldots,N_s$.
2	Prediction - predict the weights.	$w^i_{k\backslash k-1} = \sum_{j=1}^{N_s} w^j_{k-1\backslash k-1} p\left(x^i_k | x^j_{k-1}\right)$
3	Update - update the weights.	$w^i_{k\backslash k} = \frac{w^i_{k\backslash k-1} p(z_k | x^i_k)}{\sum_{j=1}^{N_s} w^j_{k\backslash k-1} p\left(z_k | x^j_k\right)}$
4	Obtain optimal minimum variance estimate of the state vector and corresponding error covariance.	$\hat{x}_k \approx \sum_{i=1}^{N_s} w^i_{k|k} x^i_k$ & $P_{\hat{x}_k} \approx \sum_{i=1}^{N_s} w^i_{k|k} (x^i_k - \hat{x}_k)(x^i_k - \hat{x}_k)^T$
5	Let k = k+1 & iterate to step 2.	

The *q_cHMM* algorithm implements a BRE smoother. BRE smoothing uses all measurements available to estimate the state of a system at a certain time or depth in the q_v estimation case. This requires both a forward and backward filter formulation. The forward HMM filter ($\hat{q}^F_k$) processes measurement data (q_c) above the cone tip ($j = 1\ to\ 30 \times \left(\frac{d_c}{\Delta}\right)$) in (1) (*N=60*)). Next the backward HMM filter ($\hat{q}^B_k$) is implemented, where the filter recurses through the data below the cone tip ($j = 30 \times \left(\frac{d_c}{\Delta}\right)\ to\ 60\left(\frac{d_c}{\Delta}\right)$ in (1) (*N=60*)) starting at the final q_c value. The optimal estimate for q_v is then defined as

$$\hat{q}^v_k = (\hat{q}^F_k + \hat{q}^B_k)/2 \quad (4)$$

where the index *k* represents each q_c measurement.

2.1.3. *CPSPE* algorithm

The *CPSPE* algorithm (Baziw, 2023a) is utilized to obtain estimates of the cone bearing blurring parameters ($z'_{50,ref}$, m_z, m_{50}, and m_q) from real data sets. This algorithm implements the Iterative Forward Modelling (IFM) parameter estimation technique. In IFM the parameters to be estimated are iteratively adjusted until a user specified cost function is minimized. The desired parameter estimates are defined as those which minimize the user specified cost function. The specific IFM technique utilized in the *CPSPE* algorithm is the downhill simplex method (DSM) (Nelder and Mead, 1965). The DSM in multidimensions has the important property of not requiring derivatives of function evaluations and it can minimize nonlinear-functions of

more than one independent variable. A simplex defines the most elementary geometric figure of a given dimension: a line in one dimension, the triangle in two dimensions, the tetrahedron in three, etc; therefore, in an N-dimensional space, the simplex is a geometric figure that consists of N+1 fully interconnected vertices.

The DSM starts at N + 1 vertices that form the initial simplex. The initial simplex vertices are chosen so that the simplex occupies a good portion of the solution space. In addition, it is also required that a scalar cost function be specified at each vertex of the simplex. The DSM searches for the minimum of the costs function by taking a series of steps, each time moving a point in the simplex away from where the cost function is largest. The simplex moves in space by variously reflecting, expanding, contracting, or shrinking. The simplex size is continuously changed and mostly diminished, so that finally it is small enough to contain the minimum with the desired accuracy

The *CPSPE* algorithm relies upon processing "well-behaved" q_c profiles. A "well-behaved" cone bearing profile is defined as containing significantly large depth intervals with known constant q_v values (greater than the transition depth uncertainties). Figure 3 illustrates a schematic of a "well-behaved" cone bearing profile. In Fig.3, known real data cone bearing measurements are available (q_{v1}, q_{v2}, q_{v3}, q_{v4}, and q_{v5}) with uncertainty in the locations of the depths (d_1, d_2, d_3, and d_4) of the interfaces (identified by light blue zones).

The *CPSPE* algorithm Cost Function (CF) to be minimized is defined as the Root Mean Square (RMS) difference between the simulated cone bearing measurements and the true cone bearing measurements. The simulated cone bearing measurements are obtained by implementing eqs. (1) and (2) for each $z'_{50,ref}$, m_z, m_{50}, m_q and depth interfaces realization. For the case illustrated in Fig. 3 there are eight unknown parameters to be estimated ($z'_{50,ref}$, m_z, m_{50}, m_q, d_1, d_2, d_3, and d_4). The *CPSPE* algorithm CF for each parameter realization is given as

$$CF = \sqrt{\sum_{z=0}^{D} \left(q_m(d) - q_c(d)\right)^2} \qquad (5)$$

where q_m is the measured cone bearing and q_c is obtained from eqs. (1) and (2) for each unknown parameter realization. D is the maximum depth of the profile.

2.2. Sleeve friction measurements

2.2.1. Sleeve friction governing equations

Sleeve friction is the measure of the average skin friction as the probe is advanced through the soil. From finite element analysis it has been shown (Susila and Hryciw, 2003) that there is a none uniform friction distribution along the length of the cone shaft. The sleeve friction close to cone tip is nearly 0 MPa and gradually increases to the uniform value 30mm to 35mm from the bottom of the shaft (Susila and Hryciw, 2003; Kiousis et al., 1988).

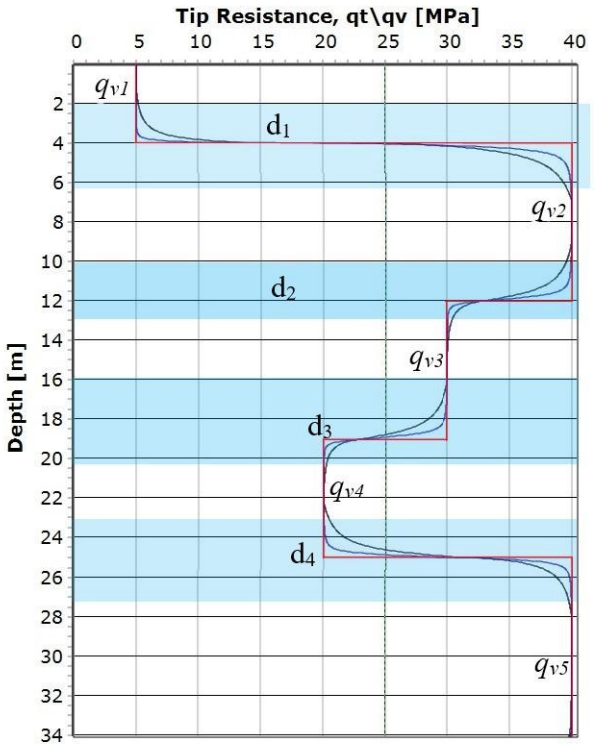

Figure 3. Example of "well-behaved" cone profile. The blue zones denote unknown transitional depths between known q_v values. The red trace is a cone bearing profile with known values (q_v). The blue trace is obtained by inputting the known red trace into eqs. (1) and (2) with the baseline values of $z'_{50,ref}$ = 4.0, m_z = 3.0, m_{50} = 0.5, and m_q = 2. The black trace is obtained by inputting the known red trace into eqs. (1) and (2) with the values of $z'_{50,ref}$ = 7.0, m_z = 2.0, m_{50} = 0.1, and m_q = 2.

The sleeve friction distribution can be thought of as a Sleeve Friction Weighting Function (SFWF) where various values of sleeve friction along the shaft (due to varying soils) are weighted to give a final measured value assumed to occur at the center of the shaft. The SFWF is mathematically approximated as (Baziw, 2023b)

$$SFWF(d^*) = 1 \; for \; d^* > 30 \; mm \qquad (6a)$$

$$SFWF(d^*) = abs(d^* - 30)^3/30^3 \; for \; d^* \leq 30 \; mm \qquad (6b)$$

where d^* = the distance from bottom of sleeve

The sleeve friction measurements f_t are generated from the true sleeve friction values f_v by implementing eq. (7) outlined below.

$$f_t(i) = \sum_{j=1}^{L^*} SFWF(j) \times f_v(i - l^* + j) \qquad (7)$$

where

Δ	sleeve friction sampling rate
L	sleeve friction shaft length
L^*	L/Δ
l	$L/2$
l^*	l/Δ

Implemention of eq. (7) requires that Δ is initially set to a 1mm sampling rate so that nearly true (i.e.,

continuous resistance along shaft) *in-situ* measurement conditions are simulated.. The simulated date sets are then obtained by extracting data from the 1mm sampling rate data sets at the user specified rate.

Table 2. CPSPE algorithm settings and optimal estimates

	$z'_{50,ref}$	m_z	m_{50}	m_q	Depth1 [m]	Depth2 [m]	Depth1 [m]	Depth2 [m]
Minimum	2	0.1	0.01	0.1				
Maximum	9	6	3	6				
Interface Transition Range					2 to 6	10 to 13	16 to 20	23 to 27
True Values	**7**	**2**	**0.1**	**2**	**4**	**12**	**19**	**25**
CPSPE Estimates	**6.8**	**2**	**0.1**	**2**	**3.9**	**12.2**	**18.9**	**24.8**

2.2.2. *OSFE-IFM* algorithm

The *OSFE-IFM* algorithm (Baziw, 2023b) is utilized to obtain estimates of the true sleeve friction values from real data sets. The *OSFE-IFM* algorithm utilizes *a posteriori* information obtained from the q_c*HMM* algorithm and implements IFM. The q_c*HMM* algorithm facilities quantifying the soil layering (i.e., layer interfaces). Soil layering can readily be quantified based upon estimated q_v values. This soil layering information is inputted into the *OSFE-HMM* algorithm.

Each of the soil layers has an associated sleeve friction values f_{v1} to f_{vN} which is estimated by IFM parameter estimation. The IFM cost function to be minimized in the *OSFE-HMM* algorithm is the RMS difference between the simulated sleeve friction values (eq. (7)) and the measured values.

3. Test bed simulations

The performances of the q_c*HMM*, *CPSPE*, and *OSFE-IFM* algorithms were evaluated by processing challenging test bed simulations. As previously outlined, it is of paramount importance that thorough test bed simulation and analysis is carried out prior to the implementation of OEAs on real data sets.

3.1. Test bed simulation of the *CPSPE* algorithm

The performance of the *CPSPE* algorithm is demonstrated by processing the challenging "well-behaved" cone bearing profile illustrated in Fig. 3. In Fig. 3, the red trace is a cone bearing profile with known values (q_v). The blue trace is obtained by inputting the known red trace into eq. (1) with the baseline values of $z'_{50,ref}$ = 4.0, m_z = 3.0, m_{50} = 0.5, and m_q = 2. The black trace is obtained by inputting the known red trace into eq. (1) with the values of $z'_{50,ref}$ = 7.0, m_z = 2.0, m_{50} = 0.1, and m_q = 2. The interface uncertainties are identified by the light blue zones and are centered around the true interfaces of d_1 = 4m, d_2 = 12m, d_3 = 19m and d_4 = 25m.

The *CPSPE* algorithm is applied on the black trace of Fig. 3 where it is initially assumed that the baseline values are valid. In this test bed simulation there are eight unknowns ($z'_{50,ref}$, m_z, m_{50}, m_q, and interfaces at d_1, d_2, d_3, and d_4). Table 2 outlines the parameters set as input into the *CPSPE* algorithm. In Table 2 the minimum and maximum values of *CBWF* parameters are specified. These limits are applied within the IFM portion of the *CPSPE*.

Table 2 outlines the uncertainty of the interface transitions for interfaces located at d_1 = 4m (2m to 6m), d_2 = 12m (10m to 13m), d_3 = 18m (16m to 20m), and d_4 = 25m (23m to 27m). In the *CPSPE* algorithm a Monte Carlo technique is utilized where the initial simplex within the IFM portion of the algorithm is initialized with cone bearing blurring parameters within the minimum and maximum ranges specified in Table 2. This Monte Carlo initialization and *CPSPE* algorithm implementation is carried out one hundred times. The *CPSPE* estimates are defined as the *CPSPE* algorithm output which results in the lowest cost function (eq. 5) from the 100 executions. Table 2 outlines the *CPSPE* optimal estimates which are nearly identical to the true values.

3.2. Test bed simulation of q_c*HMM* and *OSFE-IFM* algorithms

The performances of the *qcHMM* and *OSFE-IFM* algorithms were evaluated by processing the challenging test bed simulation illustrated in Figure 4. Figure 4 illustrates a highly variable CPT profile where it assumed that both the measured q_c and f_c have been corrected for pore pressure. In Figure 4, the true values of q_v, fv and R_{fv} are red traces while the corresponding measured values are the black traces. The black q_t measured traces were obtained by implementing eqs. (1) and (2) on the true q_v values with the true cone bearing parameters outlined in Table 1 (i.e., $z'_{50,ref}$ = 7, m_z,= 2, m_{50} = 0.1, and m_q, = 2).

Table 3 outlines the depth intervals and different SBT zones (as shown in Fig. 2) corresponding to the profiles illustrated in Fig. 4. Figure 2 illustrates the location of the 1m to 3.8m interlayering SBT zone 9 for the true values of q_v = 50MPa and f_v = 0.75MPa (**A**) and the location of the 7m to 11m interlayering SBT zone 12 for the true values of q_v = 40MPa and f_v = 2MPa (**B**). The shift of these SBT zones (**A**$'$ and **B**$'$) is also illustrated in Fig. 2 for the corresponding simulated measured q_t and f_t values.

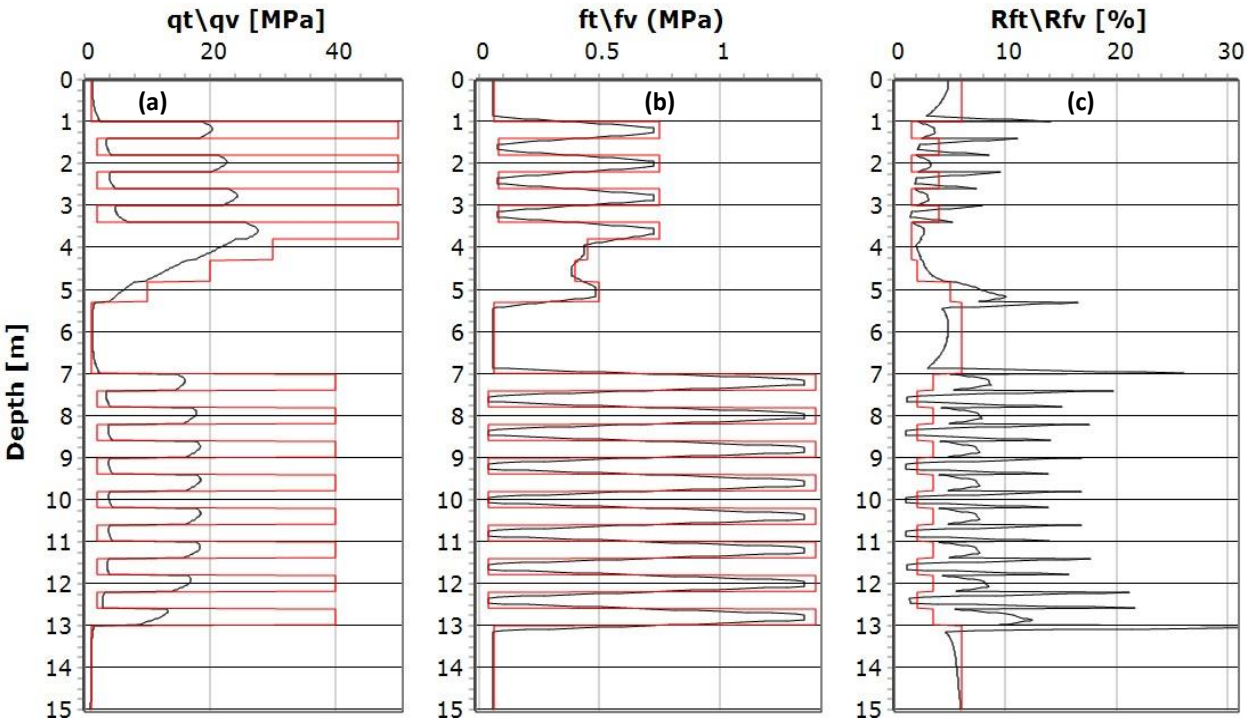

Figure 4. *qcHMM* and *OSFE-IFM* test bed simulation. (a) Simulated cone bearing data q_t (measured – black trace) and q_v (true – red trace). (b) Simulated sleeve friction data f_t (measured – black trace) and f_v (true – red trace). (c) Simulated cone friction ratio R_{ft} = 100*f_t/q_t (measured – black trace) and R_{fv} = 100*f_v/q_v (true – red trace).

Table 3. q_c*HMM* and *OSFE-IFM* test bed simulation layering and associated SBT zones.

Depth Interval [m]	q_v [MPa]	f_v [MPa]	R_v [%]	Zone
0 to 1	1	0.06	6	3
1 to 3.8 (interlayering)	50(A)/ 2	0.75(A)/ 0.08	1.5(A)/ 4	9(A)/ 4
3.8 to 4.3	30	0.45	1.5	9
4.3 to 4.8	20	0.4	2	7
4.8 to 5.3	10	0.5	5	11
5.3 to 7	1	0.06	6	3
7 to 11 (interlayering)	40(B)/ 2	2(B) /0.04	3.5(B) /2	12(B)/ 6
11 to 15	1	0.06	6	3

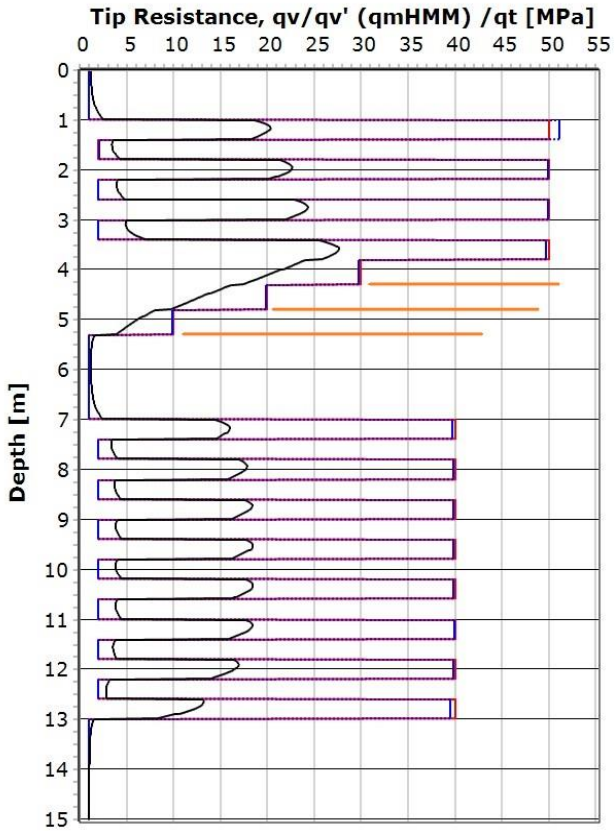

Figure 5. *qcHMM* estimated values. Red trace is the true q_v values of Fig. 4a. Black trace is the measured q_t values of Fig. 4a. Blue trace is the q_c*HMM* estimated q_v values (q_v').

Figure 5 illustrates the output from the q_cHMM algorithm after processing the measured values illustrated in Fig. 4a. The q_cHMM algorithm utilizes the estimated CPSPE algorithm blurring parameters outlined in Table 2 when processing the q_t data set. Figure 5 illustrates the test bed specified true q_v values (red line), derived measured q_t values (black line) and estimated $q_v^{/}$ values from the *qcHMM* algorithm (blue line). As is illustrated in Fig. 5, the estimated $q_v^{/}$ values are nearly identical to the true q_v values. The orange lines shown in Fig. 5 demonstrate that an investigator can readily identify the soil profile layering interfaces from the output of the q_cHMM algorithm. This *a posteriori* information is then inputted into the *OSFE-IFM* algorithm so that the associated sleeve friction values can be estimated for each soil layer identified.

Figure 6 illustrates the output from the *OSFE-IFM* algorithm after processing the measured f_t sleeve values shown in Figure 4b. In Figure 6, it is shown the test bed specified true f_v values (red line), derived measured f_t values (black line) and estimated $f_v^{/}$ values from the *OSFE-IFM* algorithm (blue line). As is illustrated in Figure 6, the estimated $f_v^{/}$ values are very close to the true f_v values.

Figure 7 illustrates friction ratio output obtained from the estimates from implementation of the *CPSPE*, q_cHMM and *OSFE-IFM* algorithms where $R_{fv}^{/}$ values are derived from $q_v^{/}$ and $f_v^{/}$ estimates. In Figure 7 the test bed specified R_{fv}, measured R_{ft} values and estimated $R_{fv}^{/}$ values are identified by red, black and blue lines, respectively. As is illustrated in Fig. 7, the estimated $R_{fv}^{/}$ values are very close to the true R_{fv} values.

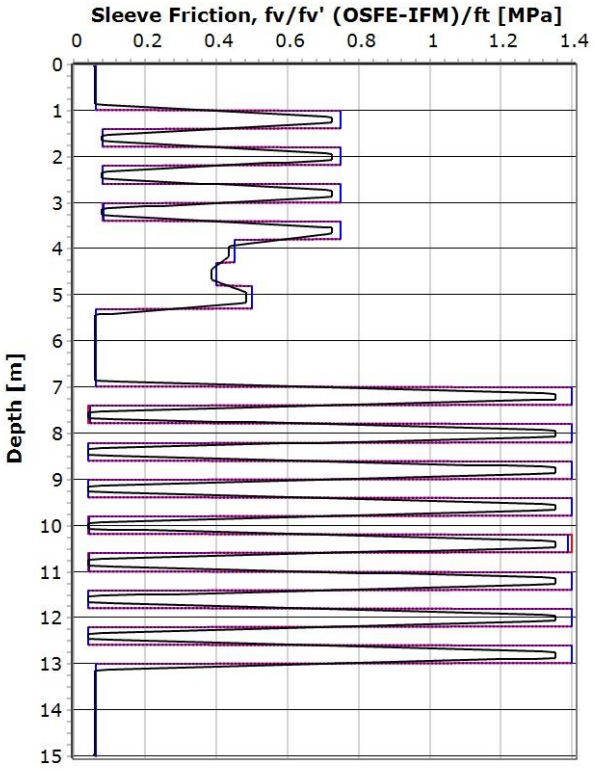

Figure 6. *OSFE-IFM* estimated values. Red trace is the true Rf_v values of Fig. 4b. Black trace is the measured f_t values of Fig. 4b. Blue trace is the *OSFE-IFM* estimated f_v values ($f_v^{/}$).

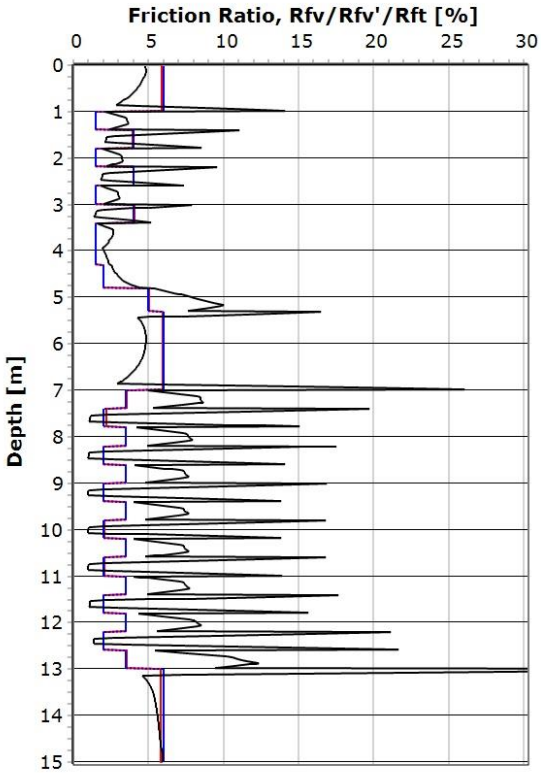

Figure 7. *qcHMM*, *CPSPE*, and *OSFE-IFM* estimated values. Red trace is the true Rf_v values of Fig. 4c. Black trace is the measured R_{ft} values of Fig. 4c. Blue trace is the q_cHMM, *CPSPE*, and *OSFE-IFM* estimated R_{fv} values ($R_{fv}^{/}$)

4. Conclusions

In CPT there can be significant blurring\smoothing of the cone bearing (q_c) and sleeve friction (f_s) measurements. There is also additive measurement noise resulting from anomalous peaks and troughs as the relatively small diameter cone tip penetrates sandy, silty and gravelly soils. It has been found that the additive measurement noise can be comparatively more challenging to remove or minimize than the smoothing effects. Cones with relatively smaller cone tips are significantly more susceptible to the anomalous peaks and troughs while cones with relatively larger tips are more susceptible to the smoothing effect.

This paper has outlined three relatively new and highly effective optimal estimation algorithms (OEAs). These algorithms are referred to as the so-called *CPSPE*, q_cHMM and *OSFE-IFM* algorithms. The *CPSPE*, q_cHMM and *OSFE-IFM* algorithms provide for the calibration of cone tips and optimal estimates of the true q_v and f_v values from the blurred measurements, respectively. The efficacy of the *CPSPE*, q_cHMM and *OSFE-IFM* algorithms was demonstrated by processing a challenging test bed simulation. Although the test bed simulation was carried out on a 40cm^2 cone, the algorithms are readily applied to q_c and f_s data acquired from a cone of any size. Furthermore, the paper is not recommending a cone of a specific size be utilized.

It is of paramount importance that the performance of newly developed OEAs is demonstrated prior to application on real data sets. It is the intentions of the

author to expand upon OEAs for CPT measurements by incorporating automated interface estimation.

References

Arulampalam, M.S., Maskell, S. and Clapp, T. 2002. "A Tutorial on Particle Filters for Online Nonlinear/Non-Gaussian Bayesian Tracking." *IEEE Transactions on Signal Processing*, 50, 174-188. https://doi.org/10.1109/78.978374

ASTM D6067/D6067M-17 (2017) Standard Practice for Using the Electronic Piezocone Penetrometer Tests for Environmental Site Characterization and Estimation of Hydraulic Conductivity. ASTM Vol. 4.09, Soil and Rock (II), D5877-Latest.

Baziw, E. and Verbeek, G. 2021a. "Implementation of Kalman Filtering Techniques for Filtering CPT Cone Bearing Measurements." The DFI 46th Annual Conference on Deep Foundations conference proceedings. October 12-15, 2021 - Las Vegas, NV. 53-67.

Baziw, E. and Verbeek, G. 2021b. "Cone Bearing Estimation Utilizing a Hybrid HMM and IFM Smoother Filter Formulation". *International Journal of Geosciences* , 12, 1040-1054. https://doi.org/10.4236/ijg.2021.1211055

Baziw, E. and Verbeek, G. 2022a. "Identification of Thin Soil Layers Utilizing the q_m*HMM-IFM* Algorithm on Cone Bearing Measurements." *Geo-Congress* 2022, Charlotte, 20-23 March 2022, 505-514. https://doi.org/10.1061/9780784484036

Baziw, E. and Verbeek, G. 2022b. "Methodology for Obtaining True Cone Bearing Estimates from Blurred and Noisy Measurements." In: Gottardi, G. and Tonni, L., Eds., Cone Penetration Testing 2022, Bologna, Italy, 115-120. https://doi.org/10.1201/9781003308829-9

Baziw, E. 2023a. "Technique for Estimating the Cone Bearing Smoothing Parameters." *International Journal of Geosciences*, 14, 603-618. https://doi.org/10.4236/ijg.2023.147032

Baziw, E. 2023b. "Methodology for Obtaining Optimal Sleeve Friction and Friction Ratio Estimates from CPT Data." International Journal of Geosciences, 14, 290-303. https://doi.org/10.4236/ijg.2023.143015

Boulanger, R.W. and DeJong, T.J. .2018. "Inverse Filtering Procedure to Correct Cone Penetration Data for Thin-Layer and Transition Effects." In: Hicks, P. and Peuchen, Eds., Cone Penetration Testing 2018, Delft University of Technology, The Netherlands, 25-44.

Kiousis, P.D., Voyiadjis, G.Z. and Tumay, M.T. 1988. "A Large Strain Theory and Its Application in the Analysis of the Cone Penetration Mechanism." *International Journal for Numerical and Analytical Methods in Geomechanics* , 12, 45-60. https://doi.org/10.1002/nag.1610120104

Lunne, T., Robertson, P. K. and Powell, J.J.M. 1997. *Cone Penetrating Testing: In Geotechnical Practice*. Taylor & Francis Group, Oxfordshire.

Nelder, J.A. and Mead, R. 1965. "A Simplex Method for Function Optimization." *Computing Journal*, 7, 308-313. https://doi.org/10.1093/comjnl/7.4.308

Robertson, P.K., Campanella, R.G., Gillespie, D. and Greig, J. 1986. "Use of Piezometer Cone Data." In -Situ '86 Use of In-Situ Testing in Geotechnical Engineering, ASCE, Reston, 1263-1280.

Robertson, P.K. and Cabal, K.L. 2012. *Guide to Cone Penetration Testing for Geotechnical Engineering*. Gregg Drilling & Testing, Inc. 5th Edition, 10.

Robertson, P.K. 1990. "Soil Classification Using the Cone Penetration Test." *Canadian Geotechnical Journal*, 27, 151-158.

Susila, E. and Hryciw, R.D. 2003. "Large Displacement FEM Modelling of the Cone Penetration Test (CPT) in Normally Consolidated Sand." *International Journal for Numerical and Analytical Methods in Geomechanics* , 27, 585-602. https://doi.org/10.1002/nag.287